Polymer Journal (2024) 56:1–16
https://doi.org/10.1038/s41428-023-00840-2

REVIEW

Structural details of carboxylic acid-based Hydrogen-bonded Organic Frameworks (HOFs)

Yuto Suzuki[1] · Ichiro Hisaki[1]

Received: 15 July 2023 / Revised: 11 August 2023 / Accepted: 15 August 2023 / Published online: 12 October 2023
© The Author(s) 2023. This article is published with open access

Abstract

Crystalline porous molecular frameworks formed through intermolecular hydrogen bonding are often called hydrogen-bonded organic frameworks (HOFs) by analogy to metal organic frameworks (MOFs) and covalent organic frameworks (COFs). Although the origin may go back to the 1960s, HOFs have recently been investigated as a new family of functional porous materials. In this review, HOFs composed of tritopic, tetratopic, and hexatopic carboxylic acid derivatives are reviewed by considering structural aspects such as isostructurality. These derivatives typically form H-bonded *hcb*, *dia*, *sql*, *hxl*, and *pcu* networks depending on the numbers, positions, and orientations of the carboxy groups in the molecule. We show detailed structures for selected HOFs indicating the low-dimensional networks formed through H-bonding of the molecule and higher-dimensional structures formed by assembly of the network. The networks can be designed and predicted from the molecular structure, while the latter is still difficult to design. We hope that this review will contribute to the well-controlled construction of HOFs.

Introduction

Crystalline porous materials made of molecular constituents networked through intermolecular hydrogen bonds (H-bonds) are termed hydrogen-bonded organic frameworks (HOFs) [1] by analogy to metal organic frameworks (MOFs) and covalent organic frameworks (COFs). Reversible bond formation frequently results in framework materials with crystallinities higher than those of other framework materials. HOFs are a subset of porous molecular crystals (PMCs) [2–9] and are particularly excellent materials from the perspective of preorganization of the frameworks. Namely, their structures are more readily designed than those of other PMCs using supramolecular synthons, which were defined by Desiraju as "structural units within supermolecules which can be formed and/or assembled by known or conceivable synthetic operations involving intermolecular interactions." [10] The frameworks assembled by H-bonding also have other names, such as supramolecular organic frameworks (SOFs) [11], noncovalent organic frameworks (nCOFs) [12], and porous organic salts (POSs) [13], depending on what structural features are of interest.

In 1969, Duchampe and Marsh reported the first crystal structure of a honeycomb network composed of 1,3,5-benzenetricarboxylic acid (trimesic acid) [14]. The molecules were networked through self-complementary H-bonded dimerization of the carboxy groups. Similarly, a H-bonded diamondoid network of adamantane-1,3,5,7-tetracarboxylic acid was reported by Ermer in 1988 [15]. These were the pioneering studies of networked supramolecular architectures using directional H-bonds, although they have no accessible pores inside the crystals due to interpenetration of the networked structures. Many H-bonded, networked architectures encapsulating solvents or other guest molecules have been reported since the 1960s as inclusion crystals made from the supramolecular synthons of 2-pyridone [16], alcohols [17], carboxylic acids [18, 19], diaminotriazine (DAT) derivatives [20], and others [21–27]. It should also be mentioned that the conventional inclusion crystals are composed of low symmetry molecules such as steroidal bile acid derivatives [28–30] and dumbbell-shaped diols [31], which provide inclusion spaces in the crystal.

✉ Ichiro Hisaki
i.hisaki.es@osaka-u.ac.jp

[1] Division of Chemistry, Graduate School of Engineering Science, Osaka University, 1-3 Machikaneyama, Toyonaka, Osaka 560-8531, Japan

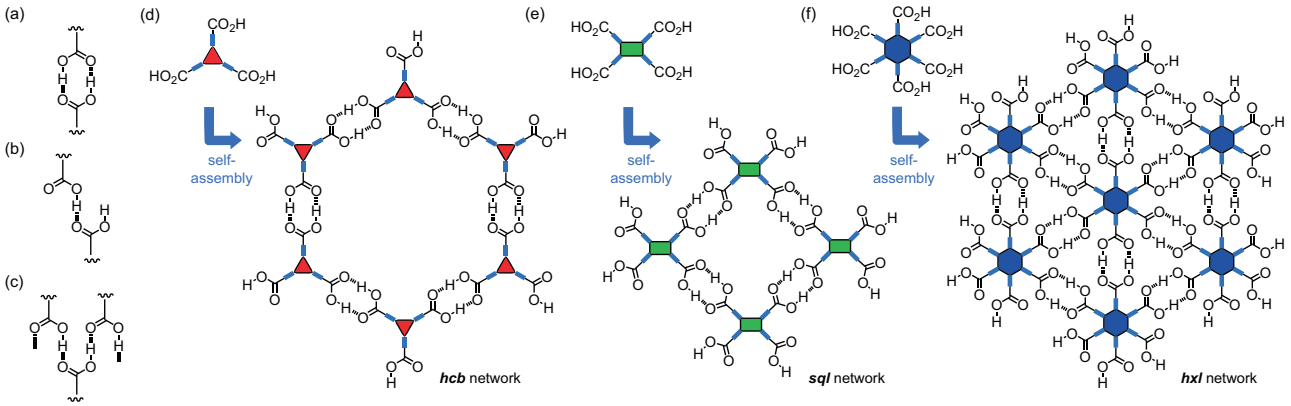

Fig. 1 Three types of typical H-bonding with carboxy groups: (**a**) complementary dimer, (**b**) truncated dimer, and (**c**) ladder-like chain bonding of carboxylic acids. (**d**) Honeycomb (*hcb*), (**e**) square (*sql*), and (**f**) hexagonal (*hxl*) topological networks composed of respective planar tritopic, tetratopic, and hexatopic carboxylic acids

In 1997, Wuest et al. reported the structure of an inclusion crystal formed from a tetraphenylmethane derivative with DAT groups [20] and implied that the crystal retained the structure after removing solvent molecules from the voids. In 2011, Chen et al. reinvestigated the porosity of the crystals and named the material **HOF-1** [1]. **HOF-1** was the first example of an HOF to demonstrate selective adsorption of C_2H_2 over C_2H_4. Since then, various HOFs have been constructed via H-bonding of various functional groups bonded to highly symmetric host molecules. The general features of HOFs are as follows:

(1) Easy to make: HOFs can be prepared via facile solvent processes, such as recrystallization and even mechanical reactions.
(2) High crystallinity: The obtained crystals have large domains with high crystallinity and are often formed as large single crystals.
(3) Reusability: The HOFs can be reuses and regenerates via solvent processes such as redissolution.
(4) Structural flexibility: Weak and reversible H-bonds provide the HOFs with structural diversity and flexibility.

Among them, structural flexibility and diversity are inextricably linked and lead to fragility and low designability. The removal of included molecules frequently causes a structural transition and consequent collapse of the structure, resulting in loss of the porosity and crystallinity. The H-bonded groups may form H-bonds with solvent molecules, resulting in the formation of unexpected, solvated, nonporous structures. This unpredictability limits the designability of HOFs. However, these issues have been overcome with design strategies, including additional use of intermolecular interactions other than H-bonding, such as π-π stacking of rigid π-conjugated skeletons or charge-assisted H-bonds formed between acidic and basic components [32, 33].

To date, several excellent review articles have been published on the design strategies, properties, and applications of HOFs [34–43]. This review, therefore, is focused on the crystallographic structural details of HOFs composed of carboxylic acid derivatives.

Carboxy groups are easily prepared by hydrolyzing esters or cyano groups. Due to these facile syntheses and moderate directivity (linearity) of the resulting H-bonded motif, the group has been used as a molecular glue for constructing supramolecular architectures. Although it forms some supramolecular synthons [10], the self-complementary dimer shown in Fig. 1a is used for HOF construction in most cases because of its high probability and designability [44, 45]. For example, it is reasonable to expect that planar tritopic, tetratopic, and hexatopic carboxylic acid derivatives can form honeycomb (***hcb***), square lattice (***sql***), and hexagonal (***hxl***) topological networks, as shown in Fig. 1d–f, respectively, where the three-letter symbols in italic bold font denote the network topology of the frameworks and have been used for classification of the frameworks [46]. Note that a H-bonded truncated dimer (Fig. 1b) or ladder-like chain (Fig. 1c) can be formed depending on the molecular structures and crystallization conditions, resulting in other types of network structures. Moreover, the molecular conformation also affects the network topology: for example, twisted tetratopic carboxylic acids tend to form HOFs with diamonded (***dia***) topological three-dimensional (3D) networks.

Tricarboxylic acids

Examples of tritopic carboxylic acid tectons include trimesic acid (**1**) [14, 18, 19, 47, 48], 1,3,5-tris(4-carboxyphenyl)benzene (**2**) [49, 50] and its derivatives **3**–**9** [51, 52] and **13** [53], tris(4-carboxyphenyl)amine (**10**) [54–57], 2,4,6-tris(4-carboxyphenyl)-1,3,5-triazine (**11**)

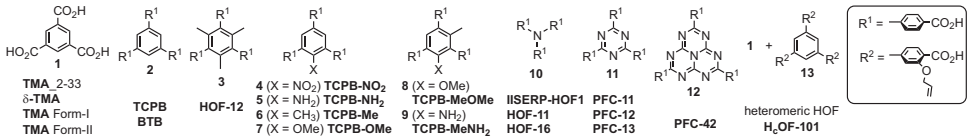

Fig. 2 Chemical structures of the tricarboxylic acid tectons that form HOFs. He names of the resultant HOFs are also presented at the bottom

[58], and 2,5,8-tris(4-carboxyphenyl)heptazine (**12**) [59], as shown in Fig. 2. Among these, C_3-symmetric molecules with planar π-conjugated cores can form H-bonded ***hcb*** networks, which are assembled with π-interactions to construct interpenetrated HOFs in many cases and non-interpenetrated layered HOFs in a few cases.

It is well known that **1** gives nonporous *C*2/*c* crystals composed of interpenetrated ***hcb*** undulated networks connected through dimerized carboxy groups. The crystal is the first structure reported for **1** [14]. Since then, a number of crystal structures have been reported for **1**, such as the non-interpenetrated layered structure with the $P3_1$ (or $P3_2$) space group reported by Herbstein et al. [18]. Also, Day and Cooper et al. discovered eight new "hidden" polymorphs and/or pseudopolymorphs of **1** using crystal structure prediction (CSP) methodology combined with robotic crystallization screening [47], and revealed that one of them, pentane-solvated **TMA_2-33** with the $P3_121$ space group, was converted to a new solvent-free HOF, **δ-TMA**, with the *C2/m* space group. **δ-TMA** had a noninterpenetrated layered structure with AB stacking (Fig. 3a). Banerjee et al. also found that the $P3_121$ crystals of **1, TMA Form II**, obtained from a THF solution had a noninterpenetrated layered structure with an ABC stacking pattern (Fig. 3b), and they demonstrated that this form converted to the interpenetrated form (**TMA Form I**) at room temperature *via* intermediate structures, which was confirmed by PXRD and FESEM analyses [48].

The HOFs composed of tectons **2** and **3**–**9** have homotypic ***hcb*** network sheet motifs formed through H-bonded dimers. However, the assembling mechanisms of the sheets differed depending on the substituted functional groups bonded to the central benzene ring. The resultant structures were categorized into four distinct types: simple stacking, single-layer offset interpenetration, double-layer offset interpenetration, and rotated-layer interpenetration. Only **7** formed a simply stacked noninterpenetrated assembly for the HOF **TCPB-OMe** (Fig. 3c) [52], while HOFs composed of tectons **3, 6**, and **7** (**HOF-12, TCPB-Me**, and **TCPB-MeOMe**, respectively) had structures with single-layer offset interpenetration, which is the most common assembly manner for the tritopic carboxylic acid tectons (Fig. 3d–f). The parallel layers slip along each other, leading to a gap into which one layer is interpenetrated. HOF **TCPB-NO_2**, on the other hand, showed a structure with double-layer offset interpenetration (Fig. 3g) [52]. HOFs **TCPB** and **TCPB-NH_2** exhibited rotated-layer interpenetration structures (Fig. 3h, i) [49, 52]. This assembly involved a two-axis interpenetration of specific layered networks, which were classified as two distinct layers (the A and B layers of simple stacking hexagonal sheets). The B layer was a rotated layer comprising the simple stacking hexagonal sheet. The B layer was rotated by 60° relative to the A layer. The number of layers varied depending on the constituent molecules: three and four layers for **TCBP** and three and three layers for **TCBP-NH_2**.

Two HOFs composed of **10** were reported, that is, **IISERP-HOF1** [54] and **HOF-11** [55], in which the carboxy groups formed H-bonded dimers. Both had almost the same porous structures with 1D channels and 11-fold interpenetrated **(10,3)-b** topological networks, although the crystallographic lattices of **IISERP-HOF1** and **HOF-11** were slightly different depending on the crystallization conditions (in acetic acid at 150 °C and in THF at room temperature, respectively). Meanwhile, the pseudopolymorphic HOF **HOF-16** [56, 57], contained carboxy groups that did not form intermolecular H-bonds, which allowed efficient separation of C_3H_6/C_3H_8 *via* interactions between the gas molecules and the free carboxy groups [57]. This pseudopolymorph provided an example of functionalization that takes advantage of the weakness of H-bonds and simultaneously showed the difficulty of constructing isostructural HOFs.

1,3,5-Triazine derivative **11** also formed a H-bonded ***hcb*** network, which, however, was not a planar ***hcb*** sheet but was undulated and polycatenated with other parallel sheets, resulting in intricate crisscrossed 3D structures (**PFC-11, -12, -13**) [58]. An undulated ***hcb*** network was also observed in the first crystal structure of **1** [14]. Heptazine derivative **12**, on the other hand, formed no **hcb** network but 1D strands, where two of the three carboxy groups in **12** formed a truncated H-bonded dimer, although the molecule was the same C_3-symmetric tritopic carboxylic acid seen in other tectons [59]. The heteromeric HOF **H_cOF-101** was obtained by cocrystallization of **1** and the *o*-alkoxycarboxylic acid derivative **13** [53]. The resultant HOF was subjected to a thiol-ene crosslinking reaction in the presence of ethanedithiol, which formed covalently linked stable porous materials.

Tetracarboxylic acids

4-Connected tectons containing four carboxy groups lying in the same plane are shown in Fig. 4. They have the planar or quasiplanar skeletons of benzene **14** [60, 61], *N*-containing polycyclic structures **15**–**17** [60–63], tetrathiafulvalene **18**

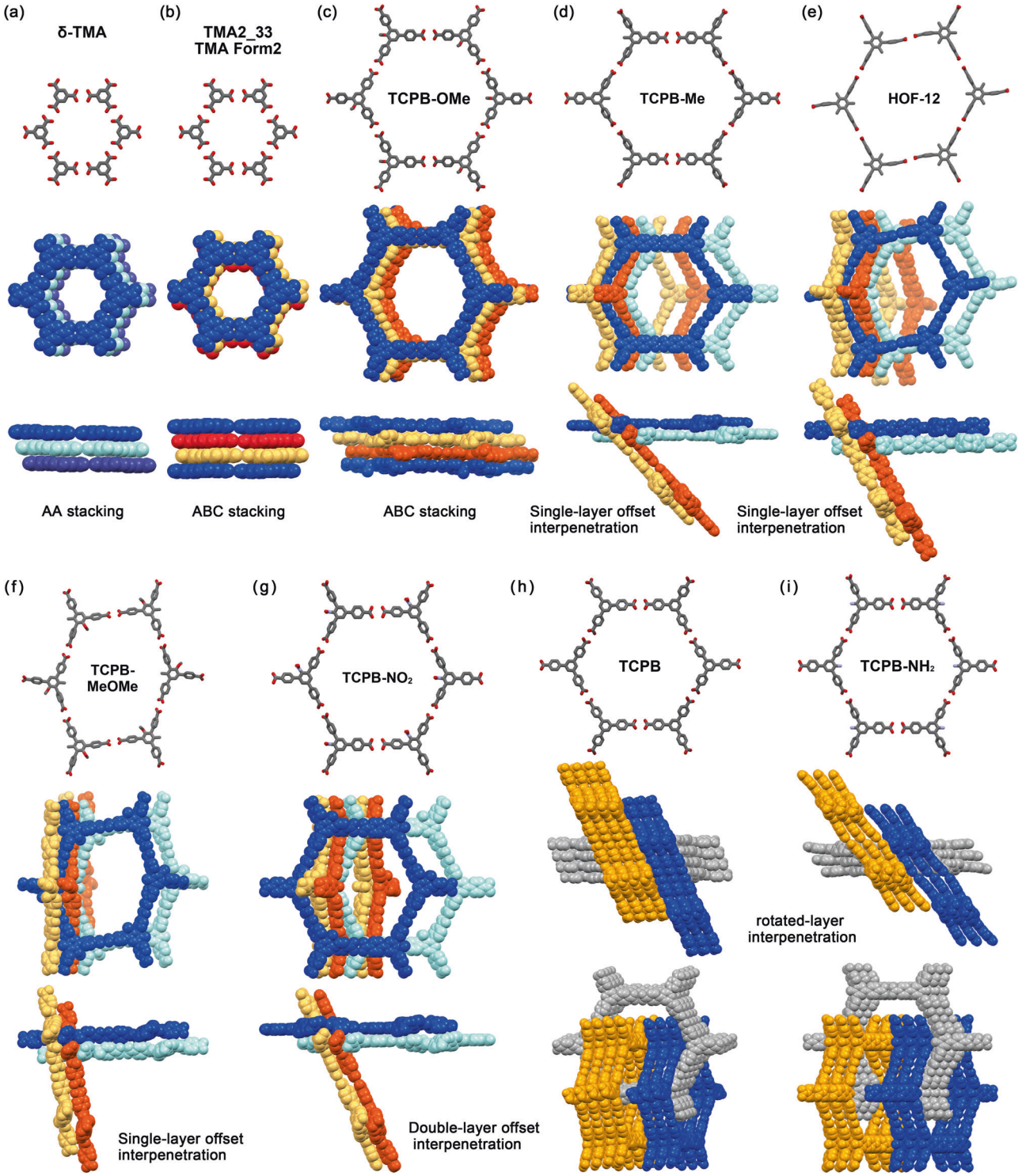

Fig. 3 Crystal structures of HOFs composed of tritopic carboxylic acids. **a** δ-TMA formed from 2, **b** TMA_2-33 or TMA Form II formed from 2, **c** TCPB-OMe formed from 7, **d** TCPB-Me formed from 6, **e** HOF-12 formed from 3, **f** TCPB-MeOMe formed from 8, **g** TCPB-NO_2 formed from 4, **h** TCPB formed from 2, and (**i**) TCPB-NH_2 formed from 5. (Top) Hexagonal network, (Middle) top view of assemblies, and (bottom) side view of assemblies. Disordered moieties were omitted for clarity

[60, 64, 65] and **19** [66], tetraphenylethene **20** [67] and **21** [68], pyrene **22**–**27** [69–72] and **32** [73], 1,2,3,6,7,8-hexahydropyrene **33** [73], porphyrin **28** [74–76], metalloporphyrin **28Co** and **28Cu** [77], and terphenyl analogs **29**–**31** [78–80].

π-Conjugated planar tectons tend to form rhombic networks with ***sql*** topologies. These homotypic networks are assembled by stacking through π-π and/or CH-π interactions to form layered frameworks. Unlike the ***hcb*** lattices formed

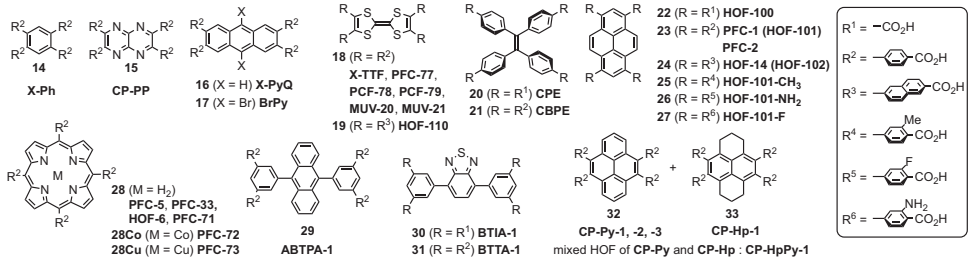

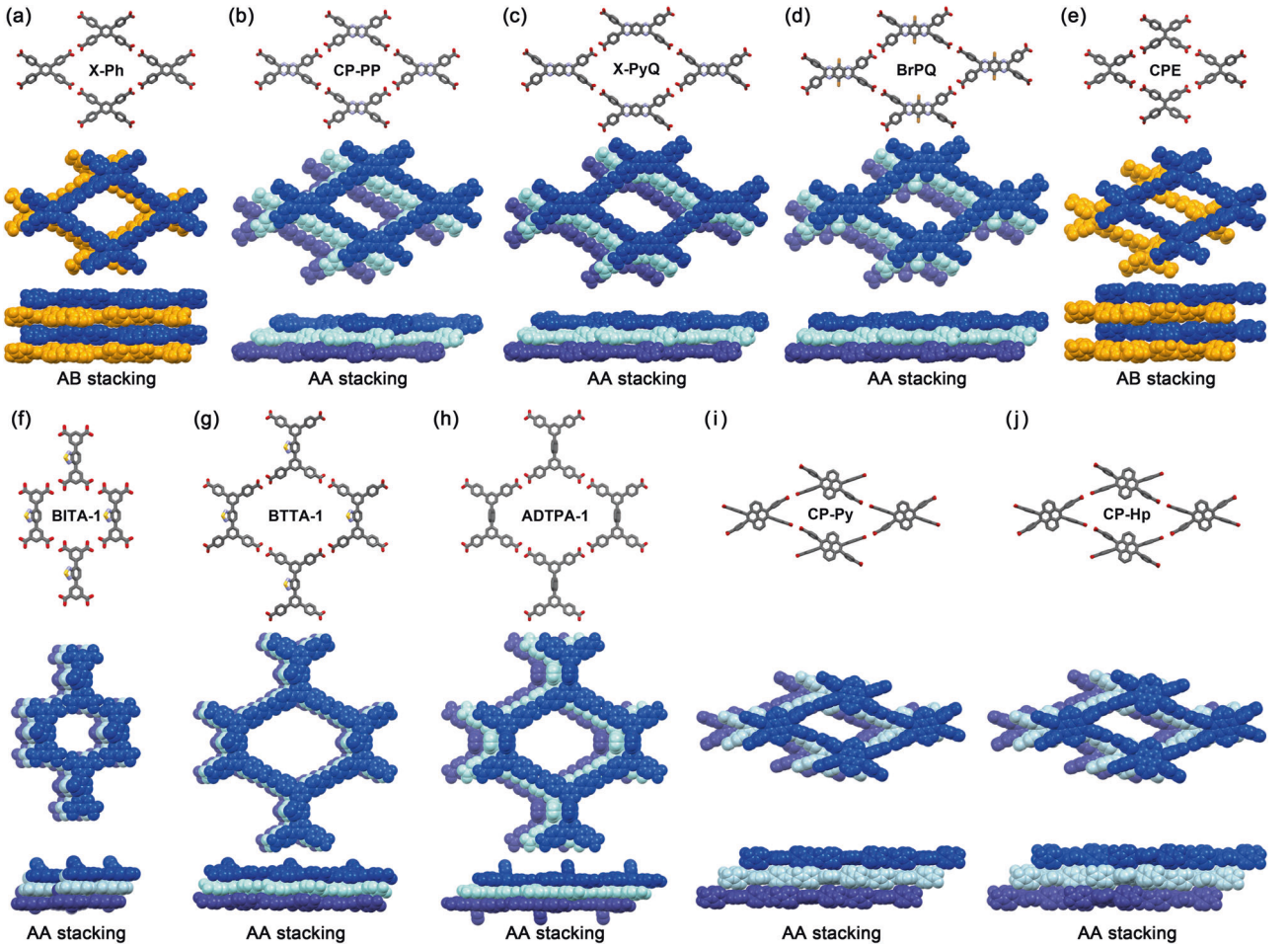

Fig. 5 Crystal structures of (**a**) X-Ph, (**b**) CP-PP, (**c**) X-PyQ, (**d**) BrPQ, (**e**) CPE, (**f**) BTIA-1, (**g**) BTTA-1, (**h**) ADTPA-1, (**i**) CP-Py, and (**j**) CP-Hp. (Top) Square-lattice networks and assembled structures, (middle) viewed down, and (bottom) viewed from the side. The disordered moieties were omitted for clarity. These structures were obtained from the SCXRD experiment except for BTIA-1, which was analyzed from the PXRD experiment. The HOF CPE in (**e**) was described only in the Supporting Information for ref. [67]

with C_3-symmetric tectons, interpenetrated structures are not common for the planar tetracarboxylic acids, presumably because of the lower symmetry of a ***sql*** network compared with that of an ***hcb*** network and/or the stabilization effect of layered stacking structures. The compounds listed in Fig. 4 basically construct 2D layered porous structures. The 2D sheets accumulate with the following nonuniform assembly manners, that is, AA stacking, AB stacking, and others, such as correlation offset stacking, resulting in the formation of nonisostructural HOFs. Tectons **14** and **20** gave the HOFs **X-Ph** [60] and **CPE** [67] with AB stacking of homotypic 2D networks (Fig. 5a, e), while tectons **15, 16, 17, 29, 30, 31** gave isostructural HOFs (**CP-PP** [62], **X-PyQ** [60], **BrPQ** [63], **ABTPA-1** [78], **BITA-1** [79], and **BTTA-1** [80], respectively) with similar AA-stacking structures (Fig. 5b–d, f–h). The HOFs **CP-PP, X-PyQ**, and **BrPQ** underwent drastic structural changes involving rearrangement of H-bonds upon removal of the accommodated solvent molecules, while the HOFs **ABTPA-1, BITA-1**, and **BTTA-1** basically retained their

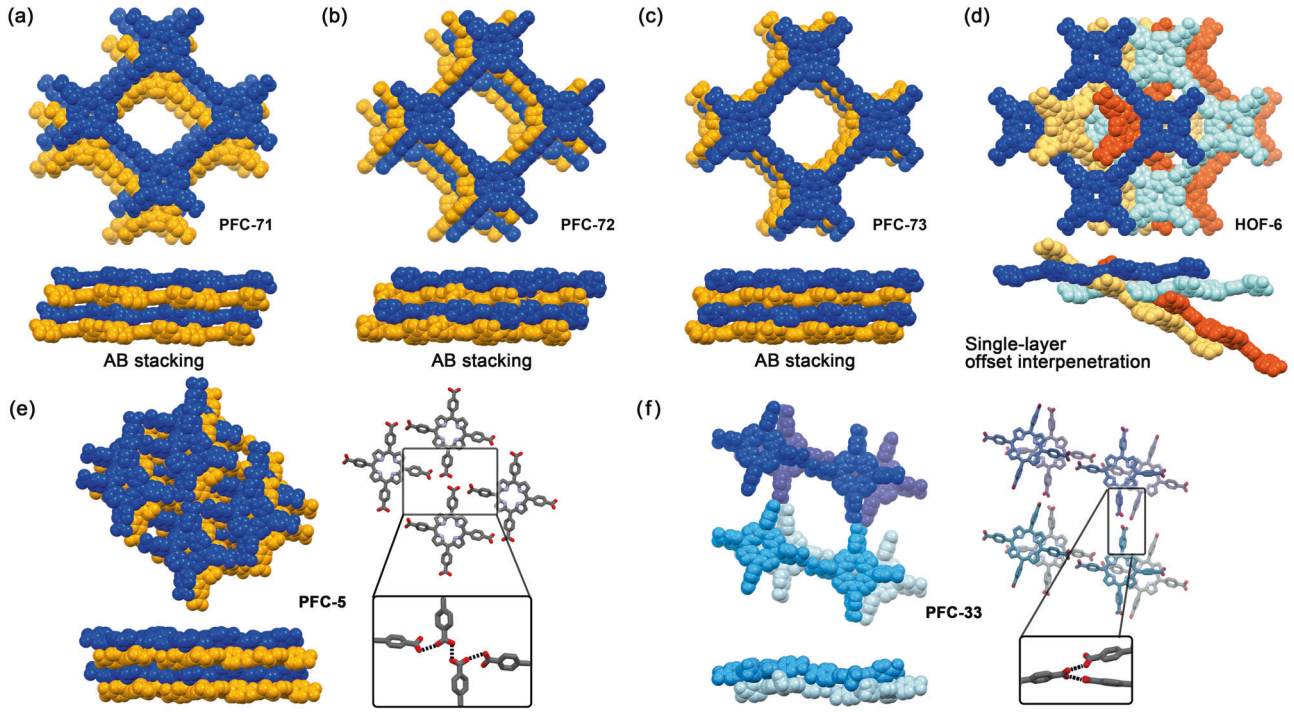

Fig. 6 Crystal structures of (**a**) PFC-71, (**b**) PFC-72, (**c**) PFC-73, (**d**) HOF-6, (**e**) PFC-5, and (**f**) PFC-33. In the case of (**e**) and (**f**), the carboxy groups formed no self-complementary dimers but branched H-bonded motifs. Disordered moieties were omitted for clarity

porous structures, except for subtle structural changes such as stacking orders and molecular conformations, and they showed Brunauer–Emmett–Teller (BET) surface areas of 1183 m^2g^{-1}, 720 m^2g^{-1}, and 1145 m^2g^{-1}, respectively. It should be noted that tecton **21** gave the HOF **CBPE**, in which **21** formed isomorphic H-bonded ***sql*** 2D sheets, and the sheets were interpenetrated three-directionally to give a ***wvm***-like weave porous structure exhibiting mechanochromic photofluorescence. It was proposed that formation of the weave structure in **CBPE** arose from the disproportionate conformation of the outer four phenylene rings in the peripheral biphenyl arms [68]. Tectons **32** and **33** yielded isostructural HOFs (**CP-Py-1** and **CP-Hp-1**, respectively) with almost identical cell parameters (Fig. 5i, j) [73]. Interestingly, the similarity of these HOFs allowed **32** and **33** to form nonstoichiometric cocrystalline frameworks (**CP-HpPy-1**) when the compounds were cocrystallized with various composition ratios. **CP-Py-1** was also revealed to exhibit static and dynamic flexibility depending on the desorption and adsorption of various guest molecules [81].

The porphyrin-based tectons **28, 28Cu**, and **28Co** formed H-bonded ***sql*** network sheets, which were stacked in an AB-stacking manner to give the series of porous frameworks **PFC-71, -72**, and **-73**, respectively. In the HOFs, the offset stacking manner of the ***sql*** networked sheets was modulated by the metal species (Fig. 6a–c), resulting in different BET surface areas (600 m^2g^{-1} for **PFC-71**, 1646 m^2g^{-1} for **PFC-72**, and 1714–1856 m^2g^{-1} for **PFC-73**) [77]. In addition to a 2D layered assembly, a 3D porous structure of the interpenetrated ***sql*** network (**HOF-6**) [74] shown in Fig. 6d and a layered porous structure (**PFC-5** [75] and **PFC-33** [76]) formed by branched H-bonds of the carboxy groups shown in Fig. 6e, f were also reported. Porphyrin-based HOFs and their composites have been used as catalysts for photooxygenation of amyloid-β [74] and for photoinduced CO_2 reduction [77] in addition to selective separation materials [75].

The formation of versatile layered HOFs was reported for TTF-based tectons **18** and **19** (Fig. 7) [60, 64–66]. In the structure of **X-TTF**, the ***sql*** layers were accumulated in the AA stacking manner, while the others were accumulated in the AB stacking manner. TTF-based HOFs underwent drastic structural changes upon solvent removal or solvent exchange, as in the cases of **CP-PP, X-PyQ**, and **BrPQ**. The PXRD changes indicated that **X-TTF** changed its framework structure upon removal of solvent molecules [60]. **PFC-77**, which was obtained from a water and THF mixed solution, transformed into **PFC-78** upon immersion in acetone, and moreover, **PFC-77** or **PFC-78** transformed into **PFC-79** with a denser framework upon immersion in dichloromethane [64]. The structure of **PFC-79** contained a tetrameric 2D H-bonded node composed of four carboxy groups, which was also formed in **BrPQ** [63]. TTF-based tectons tend to form versatile porous frameworks, such as **MUV-20a** and **MUV-20b** with the abovementioned

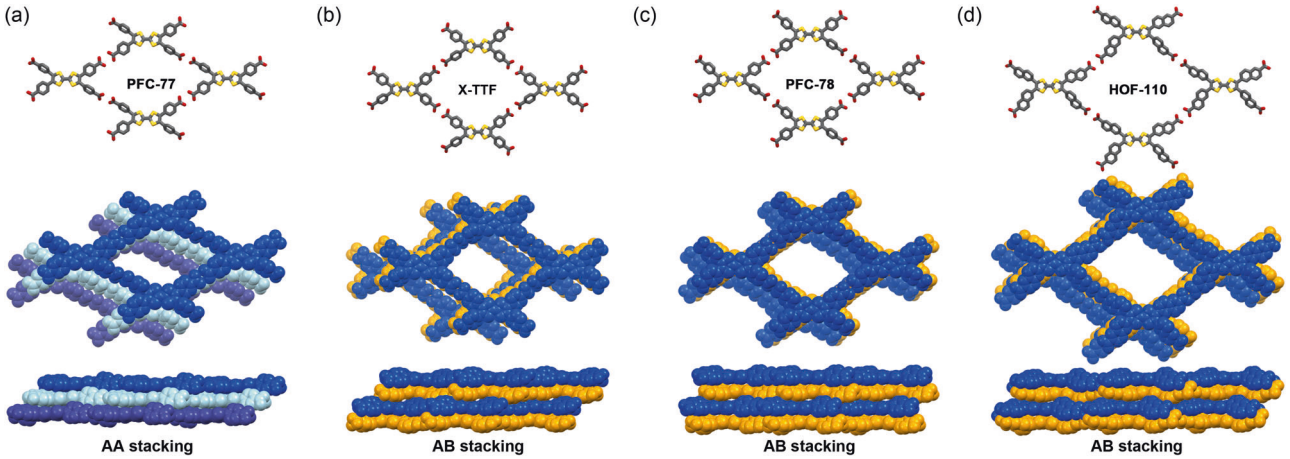

Fig. 7 Crystal structures of (**a**) PFC-77, (**b**) X-TFF, (**c**) PFC-78, and (**d**) HOF-110. Disordered moieties are omitted for clarity

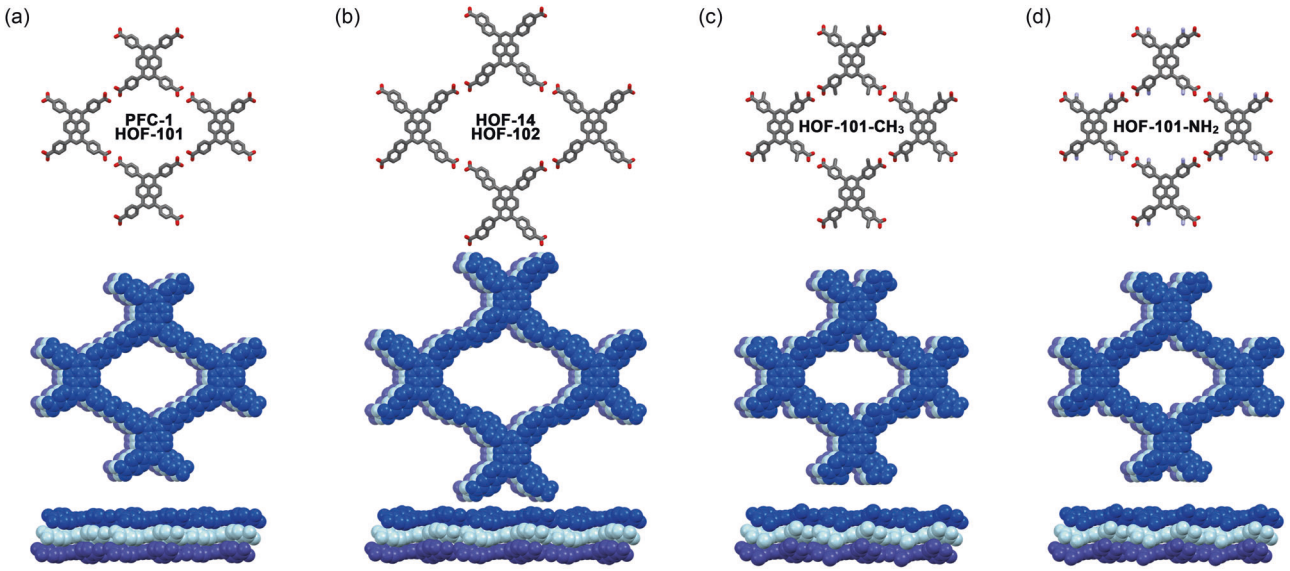

Fig. 8 Crystal structures of (**a**) PFC-1(HOF-101), (**b**) HOF-14 (HOF-102), (**c**) HOF-101-CH_3, and (**d**) HOF-101-NH_2. Disordered moieties were omitted for clarity

tetrameric node and **MUV-21** with larger honeycomb-like channels [65], the former two of which presented zwitterionic character and showed semiconduction with conductivities up to 1.35×10^{-6} Scm^{-1} [65]. TTF derivative **19** with 2-carboxynaphth-6-yl groups formed a homotypic network similar to that of **18** with 4-carboxyphenyl groups [66]. The resultant **HOF-110** showed offset stacking similar to that of **PFC-78** and became conductive after post-synthetic incorporation of iodine in the porous channels of the framework [66].

Isostructural HOFs were formed by the pyrene-based tectons **22**–**27** [69–72] via spacer modification approaches (Fig. 8). Pyrene-based tectons were reported to yield a series of isostructural HOFs with AA stacking of homotypic ***sql*** networked sheets. In 2018, Cao et al. reported that **23** gave **PFC-1**, which had a thermally and chemically stable porous framework with a BET surface area of 2122 m^2g^{-1}, and demonstrated that the HOF encapsulated doxorubicin for synergistic chemo-photodynamic therapy [70]. Li and Farha et al. reported that pyrene derivatives **23, 24, 25**, and **26** with 4-carboxyphenyl, 2-carboxynaphthyl, 3-methyl-4-carboxyphenyl, and 3-amino-4-carboxyphenyl groups, respectively, gave single-crystalline isostructural HOFs, while **22** and **27** with carboxy and 4-carboxy-3-fluorophenyl groups, respectively, gave isostructural crystalline precipitates whose structures were estimated from PXRD experiments [69, 71]. In the isostructural HOFs, the 2D ***sql*** networks were assembled by shape matching π-π stacking. Among them, **HOF-102** exhibited the largest void channel with an aperture of 2.5 nm × 3.0 nm and a BET surface area of 2500 m^2g^{-1} and was capable of adsorbing biomolecules such as cytochrome c [69]. Chen et al. also

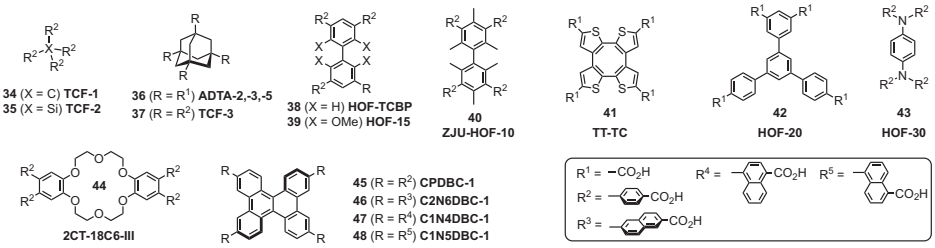

Fig. 9 Chemical structures of tetracarboxylic acids forming 3D H-bonded networked HOFs. Names of the resultant HOFs are also presented in bold

reported that **24** yielded **HOF-14** with high stability and porosity [72]. **HOFs-101-CH_3**, **-NH_2**, and **-F** were reported as chemically engineered frameworks of **HOF-101**. **HOF-101-F** showed a 10- to 60-fold enhancement in the generation of reactive oxygen species (ROS) and a 10- to 20-fold greater ROS storage ability compared to traditional TiO_2 and C_3N_4 self-cleaning materials [71]. From a structural perspective, **HOF-103-CH_3** and **-NH_2** had slightly longer interlayer distances and offsets due to their steric hindrance (former: 3.42 Å and 1.71 Å, latter: 3.46 and 1.73 Å), and those lengths in **PFC-1** and **HOF-14** were similar (former: 3.39 Å and 1.65 Å, latter: 3.40 and 1.67 Å). Tecton **23** was also reported to give Kagome-like isomeric HOF **PFC-2** containing a large channel with a diameter of 2.97 nm [81]. Interestingly, single crystals of **PFC-2** were obtained by recrystallization of **23** from a DMF and ethanol solution at 90 °C in the presence of equimolar 1,4-bis(4-(3,5-dicyano-2,6-dipyridyl)dihydropyridyl)-phenylbenzene (L_2), while only a crystalline powder was formed without L_2 [81]. In contrast with 1,3,6,8-substituted pyrene derivatives such as **23**, 4,5,9,11-substituted pyrene derivative **32** gave a flexible HOF because the substituent aryl groups prevented the pyrene core from π-π stacking: **CP-Py-1** was transformed into **CP-Py-3** *via* **CP-Py-2** through shrinkage of the framework and rearrangements of the H-bonds [82].

4-Connected tectons containing four non-coplanar carboxy groups are shown in Fig. 9. Tectons with the cores methane **34** [83], silane **35** [83], and adamantane **36** [47] and **37** [83] have tetrahedral (T_4) symmetry. Others have twisted and/or nonplanar skeletons, as with biphenyls **38**–**40** [61, 84–86], tetra[2,3]thienylene **41** [87], 5'-phenyl-*m*-terphenyl **42** [88], *p*-phenylenediamine **43** [89], 18-crown-6-ether **44** [90], and dibenzo[g,p]chrysene **45**–**48** [91, 92]. Most of these nonplanar tetratopic tectons form diamonded (***dia***) topological networks through H-bonding, and assembly of the networks also proceeded in parallel with the networking through weaker noncovalent interactions, such as van der Waals interactions, to give interpenetrated frameworks. When the single H-bonded network has an inside pore larger than the size of the molecular components, additional networks are formed in the pore, leading to the formation of interpenetrated, less porous framework structures. Homotypic networks are easily obtained from complementary H-bonded dimers of carboxy groups, while the entire structures are not always isostructural because interactions between the networks depend on the molecular structure.

T_4-symmetric tectons **34**–**37** formed ***dia*** topological H-bonded networks, which assembled into interpenetrated HOFs through nondirectional weak interactions. Tectons **34** and **35** gave the corresponding porous HOFs **TCF-1** and **TCF-2**, both of which showed 6-fold interpenetrated ***dia*** networks. On the other hand, **TCF-1** had 1D channels, while **TCF-2** had 3D-networked channels, depending on the interpenetration manner of the single network [83]. CSP screening was successfully applied with **36** to experimentally observe the solvated HOFs **ADTA-2** and **3** with 2-fold and 3-fold interpenetration, respectively, in addition to the known form with 5-fold interpenetration [47]. Expanded tecton **37**, on the other hand, gave the nonporous structure **TCF-3**, in which the presence of THF molecules disrupted the formation of H-bonded dimers by the carboxy groups [83]. Since there are no directional interactions in the networks of non-π-conjugated molecules, the assembly manner is readily variable depending on the molecular structure, guest molecules, and crystallization conditions, resulting in a wide variety of porous structures. Moreover, even if they exhibited persistent porosity, they often underwent structural transitions after guest removal.

Tectons **38**–**40** formed H-bonded, three-dimensionally networked frameworks because of the twisted conformations of their sterically hindered biphenyl cores. Their HOFs, **HOF-TCBP, ZJU-HOF-10**, and **HOF-15**, showed the same ***dia*** topological network, while the shape, assembly manner, and number of interpenetrated network structures depended on the substituent groups. Pristine tecton **38** exhibited π-π stacking in the 5-fold interpenetrated **HOF-TCBP** (Fig. 10a) [84], while the methyl and methoxy substituents in **39** and **40**, respectively, forced the central biphenyl moieties to assemble via CH-π interactions instead of π-π interactions, resulting in the 6-fold and 7-fold interpenetrated HOFs **ZJU-HOF-10** [86] and **HOF-15** [85], respectively (Fig. 10b, c). Tecton **41** formed the 6-fold interpenetrated HOF **TT-TC**, in which ***dia*** network structures were assembled by π-π stacking (Fig. 10d) [87]. Interestingly, a change in the molecular structure of **41** triggered by the removal of the solvent molecules resulted in jumping behavior of the HOF crystals. The

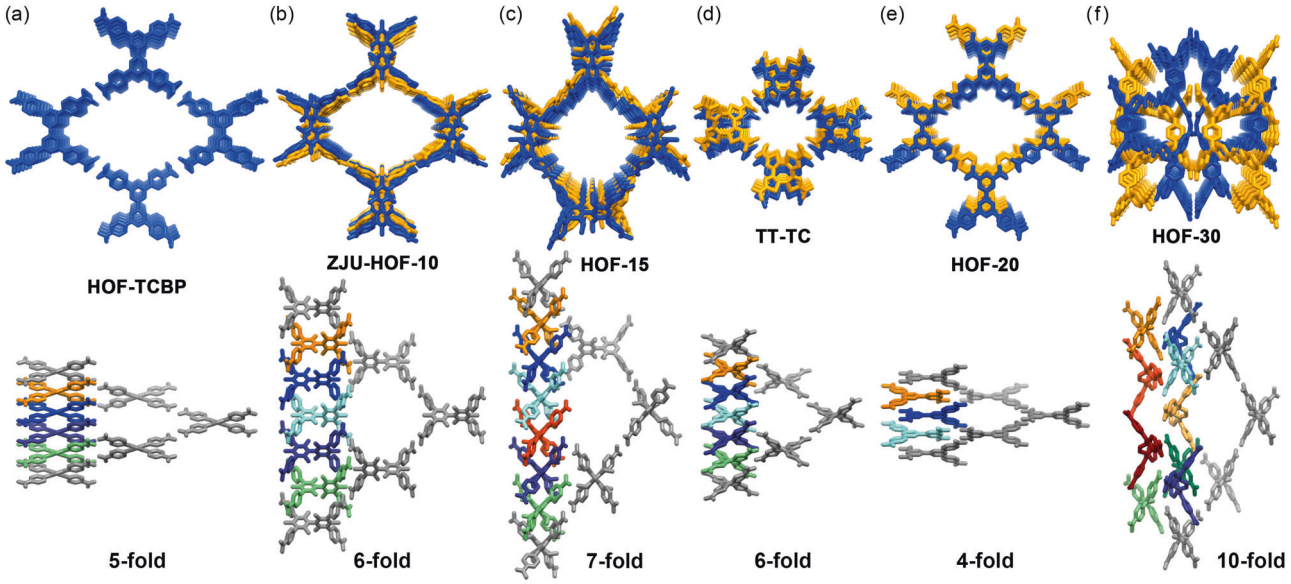

Fig. 10 Crystal structures of (**a**) **HOF-TCBP**, (**b**) **ZJU-HOF-10**, (**c**) **HOF-15**, (**d**) **TT-TF**, (**e**) **HOF-20**, and (**f**) **HOF-30** with 5-, 6-, 7, 6-, 4-, and 10-fold interpenetrated frameworks. (Top) Assembled porous structures and (Bottom) a single ***dia***-network colored gray and 1D assembled columnar structures, for which the number of colors in the stacked molecules correspond to the number of interpenetrated frameworks. Guest molecules and disordered moieties were omitted for clarity

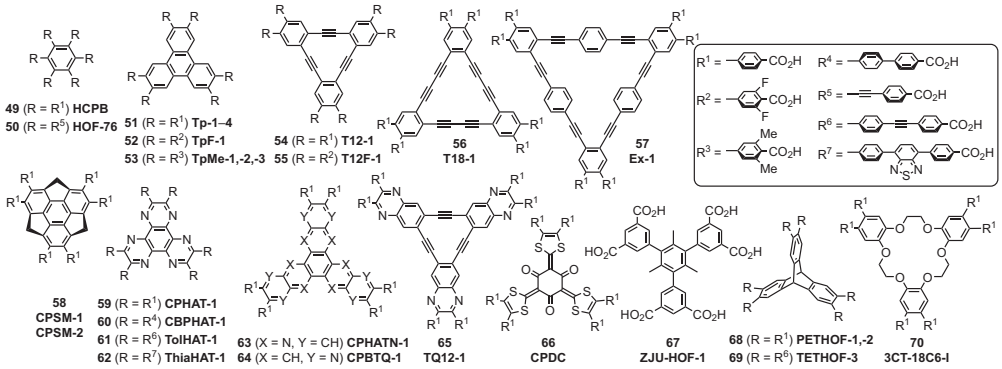

Fig. 11 Chemical structures of hexatropic carboxylic acids forming HOFs. Names of the resultant HOFs are also presented in bold

heterobiphenyl tecton **42** with carboxy and 4-carboxyphenyl groups gave **HOF-20**, which had a 4-fold interpenetrated ***ThSi2*** topological H-bonded network (Fig. 10e) [88]. **HOF-20** exhibited efficient turn-up fluorescent sensing of aniline in water with a detection limit of 2.24 μM. Tecton **43** had *p*-phenylenediamine moieties with a perpendicular orientation of the phenylene core relative to the amine moieties and formed the 10-fold interpenetrated framework **HOF-30** with a topological H-bonded network (Fig. 10f) [89]. Tecton **44** included a flexible 18-crown-6-ether moiety, and therefore, the resultant HOF **2CT-18C6-III** was nonporous, and the H-bonded network in the HOF was very complicated [90]. Tectons **45**–**48** had dibenzo[g,p]chrysene cores and formed robust 1D stacked columnar structures due to shape-filled docking of the twisted π-conjugated skeleton, which gave the isostructural porous HOFs **CPDBC-1** [91], **C1N4DBC-1, C1N5DBC-1**, and **C2N6DBC-1** [92]. Although the structures of their solvated frameworks were similar, their dynamic behaviors during desorption and adsorption of solvent molecules were different depending on the chemical structures of the spacer moieties.

Hexacarboxylic acids

The molecular structures of hexatopic tectons are shown in Fig. 11. They typically have π-conjugated cores with benzene **49** [93], **50** [94], and **67** [95], triphenylene **51** [96], **52** [97], and **53** [97], acetylene bridged macrocycles **54** [98], **55** [99], **56** [98, 100], and **57** [98], bowl-shaped sumanene **58** [101], hexaazatriphenylene (HAT) **59** [102], **60** [103],

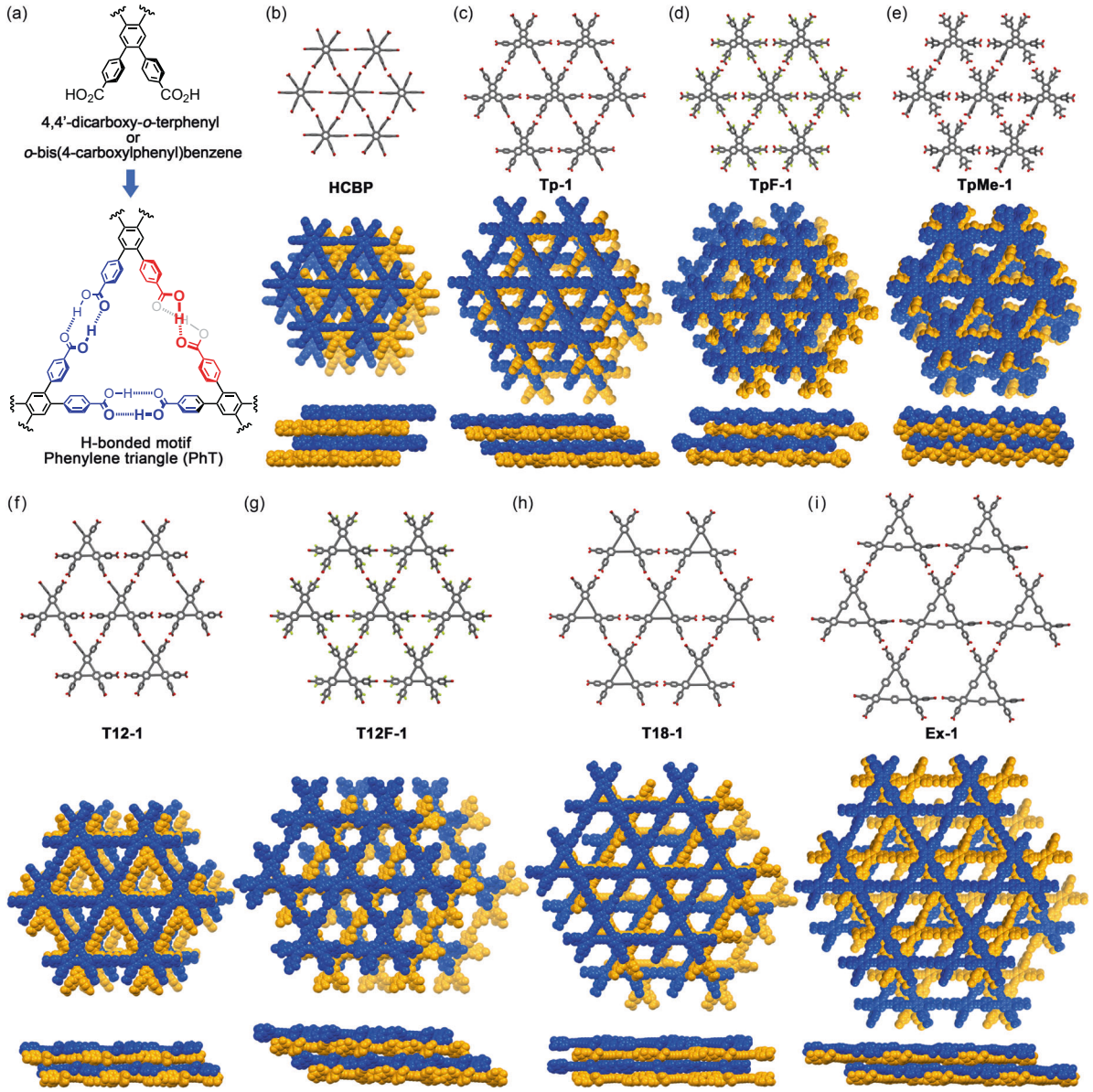

Fig. 12 **a** H-bonded motif, the so-called phenylene triangle (PhT), formed from 4,4'-*o*-terphenyl moieties. Crystal structures of HOFs possessing layered hexagonal network structures: (**b**) **HCBP**, (**c**) **Tp-1**, (**d**) **TpF-1**, (**e**) **TpMe-1**, (**f**) **T12-1**, (**g**) **T12F-1**, (**h**) **T18-1**, and (**i**) **Ex-1**. Hexagonal network; in (**a**), the PhT motif contains at least one twisted H-bonded dimer due to conformational frustration. Guest molecules were omitted for clarity

61 [104], and **62** [104], hexaazatrinaphthylene (HATN) **63** [105], benzotriquinoxaline **64** [106], quinoxaline-annelated dehydro[12]annulene **65** [107], tri(dithiolylidene)cyclohexanetrione **66** [108], and triptycene **68** [109] and **69** [110], as well as 18-crown-6-ether **70** [111].

These tectons have 4,4'-dicarboxy-*o*-terphenyl and analogous substructures, which form robust H-bonded cyclic trimers, or so-called phenylene triangles (PhT) (Fig. 12a). Formation of a PhT motif consequently results in expansion of the ***hxl*** topological hexagonal network. Tectons with planar π-conjugated hydrocarbon cores (**49, 51, 52, 53, 54, 55, 56**, and **57**) and those with a planar N-hetero π-conjugated core (**63**) formed homotypic ***hlx*** sheets, which were stacked in an inverted fashion through π-π, CH-π and CH-O interactions to give noninterpenetrated, layered HOFs with AB stacking, although optimization of the recrystallization conditions, such as the temperature and the combination of solvents, was needed. The resulting offset arrangements of the AB stacked layers, on the other hand, differed from each other depending on the core structures [98] and substituents at the *ortho*-positions relative to the carboxy groups [97, 99].

Kobayashi et al. reported the first crystal structure of a layered ***hlx*** network with hexasubstituted benzene

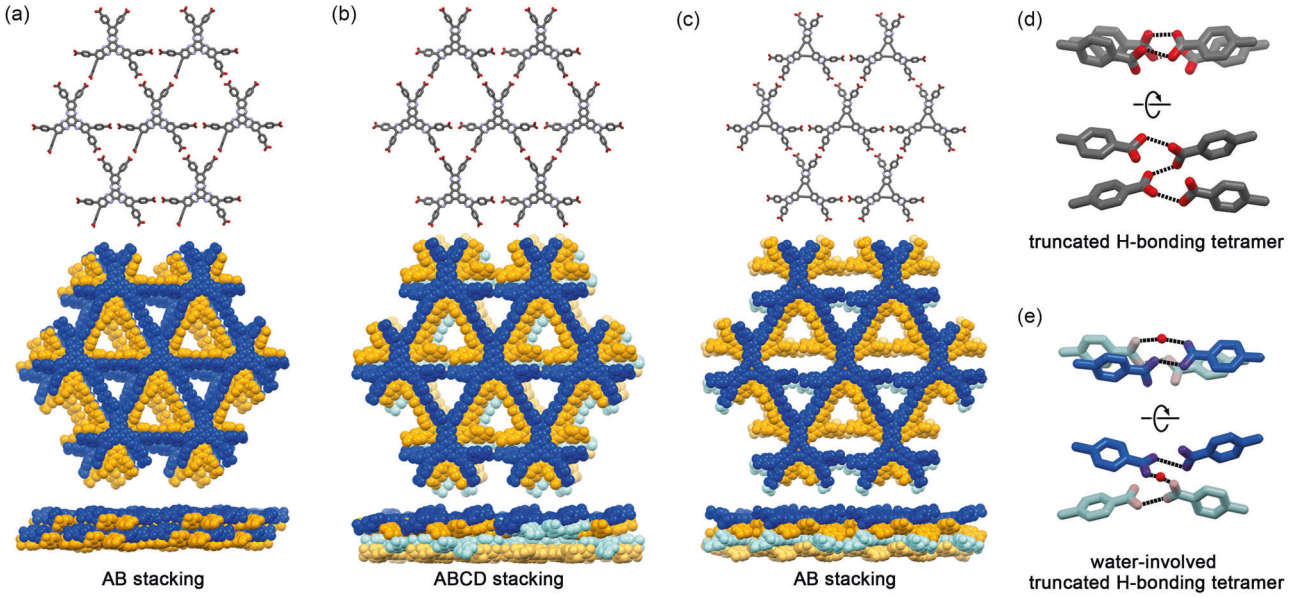

Fig. 13 Crystal structures of (**a**) CPHATN-1, (**b**) CPBTQ-1, and (**c**) TQ12-1. (top) Hexagonal networks and assembled structure (middle) viewed down and (bottom) viewed from the side. **d** Interlayer H-bonds with the truncated tetramer fashion observed in CPBTQ-1. **e** Interlayer H-bonds with the water-incorporated truncated tetramer observed in TQ12-1. Guest molecules and disordered moieties were omitted for clarity

derivative **49**. The crystals of the HOF **HCPB** were obtained by recrystallization from methanol solution with and without the guest molecule 2,7-dimethoxynaphthalene. In the crystal structure, the peripheral phenylene groups of **49** were almost perpendicular to the central benzene ring due to steric hindrance, which resulted in a longer interlayer distance of 5.6 Å for the HOF [93]. Triphenylene-based tecton **51** formed four polymorphic HOFs, **Tp-1, -2, -3**, and **-4** [96]. Generation of the polymorphs originated from versatile locations and conformational frustration of the PhT moieties: namely, adjacent peripheral phenylene groups of the 4,4'-dicarboxy-*o*-terphenyl in **51** were inclined in the same direction to avoid steric repulsion between them, and therefore, the PhT motif included at least one conformationally frustrated H-bonded carboxyl dimer, as shown in Fig. 12a [96]. The activated HOF **Tp-a**, which was characterized by a combination of CSP and experimental PXRD measurements, exhibited permanent porosity with a BET surface area of 718 m^2g^{-1} [98]. The triphenylene-based tecton **52** also gave polymorphic HOFs with layered ***hlx*** sheets (**TpMe-1, -2**, and **-3**) due to the versatile conformations of the sterically hindered peripheral groups [97]. Tecton **53** gave the HOF **TpF-1**, in which the peripheral groups were disordered in two positions due to steric hindrance [97]. The π-conjugated cyclic tectons **54, 55, 56**, and **57** formed homotypic ***hlx*** sheets with scalene hexagonal apertures, and the longer side lengths ranged from 4.6 to 11.4 Å depending on the size of the macrocycle [98]. The resultant HOFs **T12-1, T18-1**, and **Ex-1** had solvent accessible voids of 41%, 58%, and 59%, respectively, calculated by PLATON software with a proven radius of 1.2 Å. After activation, **T12-1** retained its crystallinity and permanent porosity with a BET surface area of 557 m^2g^{-1} and showed reversible dynamic structural changes among four different crystalline states during CO_2 sorption [112]. The photodynanic behaviors of HOFs **T12-1** and **Ex-1** were also investigated by Douhal et al. with fluorescence microscopy applied to single HOF crystals [113, 114].

HATN derivative **63** gave the HOF **CPHATN-1a** with a BET surface area of 379 m^2g^{-1} (Fig. 13a). Upon exposure to acids such as HCl, **CPHATN-1a** changed color from yellow to reddish brown, and the original color was recovered when the acid was removed [105]. Wang and Jiang et al. applied **CPHATN-1a** as a cathode material in a lithium-ion battery [115]. Analogs **64** [106] and **65** [107] formed the layered HOFs **CPBTQ-1** and **TQ12-1** with quasi ***hlx*** structures (Fig. 13b, c), in which the carboxy groups formed truncated interlayer H-bonds as well as the complementary dimer (Fig. 13d, e). In particular, **64** formed a complicated, low-symmetry, layered structure with ABCD stacking [106]. **CPBTQ-1** and **TQ12-1** also showed color changes from yellow to reddish brown upon exposure to HCl due to the proton-responsive pyrazine rings incorporated in the π-conjugated systems.

When a tecton with a bowl-shaped π-conjugated core is used to construct a HOF, the resultant H-bonded network differs drastically from those composed of planar tectons. The sumanene derivative **58** gave two HOFs, **CPSM-1** and **CPSM-2**; the former had a layered structure composed of

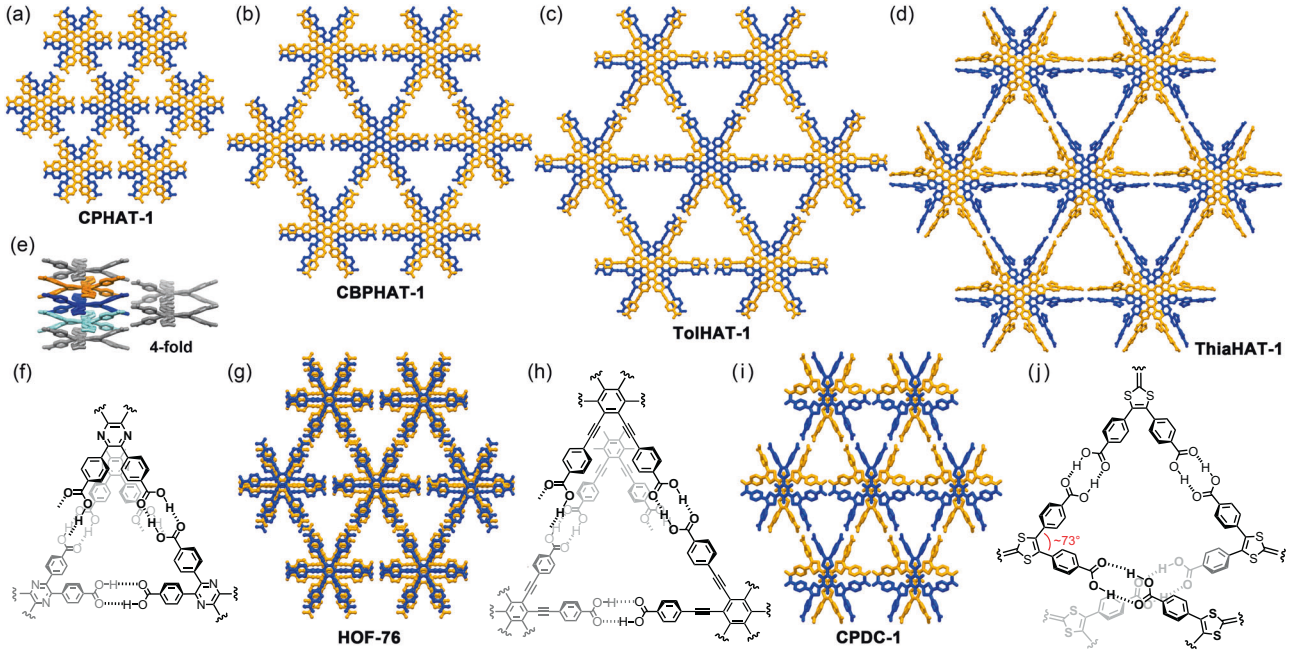

Fig. 14 Crystal structures of HOFs with helical H-bonded strands; (**a**) CPHAT-1, (**b**) CBPHAT-1, (**c**) TolHAT-1, (**d**) ThiaHAT-1, (**g**) HOF-76, and (**i**) CPDC-1. **e** Selected side view of the 4-fold interpenetrated framework of CPHAT-1. Schematic representation of helical H-bonding in (**f**) CPHAT-1, (**h**) HOF-76, and (**j**) CPDC-1. Guest molecules were omitted for clarity

ungulated ***hlx*** sheets, while the latter had exotic bilayered structures with a complicated topological network formed through an H-bonded trefoil knot [101]. Even when using a tecton whose π-conjugated core was apparently flat, the resultant HOF may have a three-dimensionally networked framework. For example, HAT derivative **59** exhibited a nonplanar propeller-shaped twisted conformation in the crystalline state, probably due to the packing force, which resulted in the formation of a 3D ***pcu*** network through helical H-bonds instead of a 2D ***hxl*** network (Fig. 14a, e, f) [102]. The 3D networked structures were assembled uniformly through π-stacking to form a 4-fold interpenetrated porous structure. Importantly, the twisted cores stacked in a shape-fitted fashion to yield a robust 1D columnar architecture, which played a role in stabilizing the HOF. Indeed, the activated HOF **CPHAT-1a** retained single crystallinity and exhibited a BET surface area of 649 m^2g^{-1} and heat resistance up to 339 °C. A series of HAT derivatives **60, 61**, and **61** also formed the isostructural HOFs **CBPHAT-1, TolHAT-1**, and **ThiaHAT-1**, respectively (Fig. 14b–d), which had 6-, 8-, and 8-fold interpenetrated structures with the same ***pcu*** topological network, and the pore sizes were determined by the arms with different lengths [103, 104]. The BET surface areas of the HAT systems ranged from 649 m^2g^{-1} to 1394 m^2g^{-1}. These HOFs also showed HCl-induced color changes due to the pyrazine rings incorporated in the π-conjugated cores [104, 116]. The hexa-substituted benzene derivative **50** formed **HOF-76** with a ***pcu*** network without interpenetration due to the slightly twisted molecular conformation (Fig. 14g, h). The HOF exhibited a BET surface area of 1100 m^2g^{-1} and showed preferential binding of C_2H_6 over C_2H_4 and thus highly selective separation of C_2H_6/C_2H_4 mixtures [94]. The HOF **CPDC-1** was constructed from the bis(4-carboxyphenyl)dithiol-based tecton **66**, in which the angle between the two 4-carboxyphenyl groups was *ca.* 73° (Fig. 14i, j) [108]. The angle was smaller than that of the 4,4'-dicarboxy-*o*-terphenyl group. Therefore, **66** formed an anomalistic, noninterpenetrated, helical network denoted by the $\{8^2.10\}$ point symbol instead of a ***hxl*** or ***pcu*** network. Tecton **67** formed the 3-fold interpenetrated HOF **ZJU-HOF-1** with a BET surface area of 1465 $m^2\,g^{-1}$, which showed a high C_2H_6 uptake capacity and excellent C_2H_6/C_2H_4 selectivity [95]. Another type of hexatropic tectonism is triptycene-based tectonism. Tecton **68** formed the polymorphic HOFs **PETHOF-1** and **PETHOF-2**, in which a single network exhibited the same hexagonal topology ***acs***, while the network was interpenetrated in different ways to form two kinds of HOFs [109]. The tecton **69** yielded the HOF **PETHOF-3** with a topological network unlike those of the former two [110]. The 18-crown-6-ether tecton **70** yielded the HOF **3CT-18C6-I** possessing a layered structure with hexagonally networked 2D sheets [111].

Conclusion

In this review, we reviewed hydrogen-bonded frameworks (HOFs) composed of tritopic, tetratopic, and hexatopic

carboxylic acid derivatives from a structural perspective. Since the carboxy groups formed predictable linear dimers through reversible H-bonding in many cases, the dimers were applied as supramolecular synthons to construct designed networked structures; for example, tritopic planar tectons can give an ***hcb*** network, nonplanar and planar-shaped tetratopic tectons can give ***dia*** and ***sql*** networks, respectively, and planar hexatopic tectons can give an ***hxl*** network. The higher dimensional structures formed by assembling the network structure, however, are still difficult to design due to the weaker and less-directional interactions between the networks. Moreover, even slight distortion of the tectons results in the formation of unpredicted networks, such as the ***pcu*** network formed by apparently planar hexasubstituted tectons. Therefore, these two issues are the next topics to be resolved for well-controlled construction of HOFs.

Funding Open access funding provided by Osaka University.

Compliance with ethical standards

Conflict of interest The authors declare no competing interests.

Publisher's note Springer Nature remains neutral with regard to jurisdictional claims in published maps and institutional affiliations.

Open Access This article is licensed under a Creative Commons Attribution 4.0 International License, which permits use, sharing, adaptation, distribution and reproduction in any medium or format, as long as you give appropriate credit to the original author(s) and the source, provide a link to the Creative Commons licence, and indicate if changes were made. The images or other third party material in this article are included in the article's Creative Commons licence, unless indicated otherwise in a credit line to the material. If material is not included in the article's Creative Commons licence and your intended use is not permitted by statutory regulation or exceeds the permitted use, you will need to obtain permission directly from the copyright holder. To view a copy of this licence, visit http://creativecommons.org/licenses/by/4.0/.

References

1. He Y, Xiang S, Chen B. A microporous hydrogen-bonded organic framework for highly selective C_2H_2/C_2H_4 separation at ambient temperature. J Am Chem Soc. 2011;133:14570–3.
2. Sozzani P, Bracco S, Comotti A, Ferretti L, Simonutti R. Methane and carbon dioxide storage in a porous van der Waals crystal. Angew Chem Int Ed. 2005;44:1816–20.
3. Bezzu CG, Burt LA, McMonagle CJ, Moggach SA, Kariuki BM, Allan DR, et al. Highly stable fullerene-based porous molecular crystals with open metal sites. Nat Mater. 2019;18:740–5.
4. Barbour LJ. Crystal porosity and the burden of proof. Chem Commun. 2006;42:1163–8.
5. Mastalerz M. Permanent porous materials from discrete organic molecules–towards ultra-high surface areas. Chem Eur J. 2012;18:10082–91.
6. Hashim MI, Hsu CW, Le HTM, Miljanić OS. Organic molecules with porous crystal structures. Synlett. 2016;27:1907–18.
7. Cooper AI. Porous molecular solids and liquids. ACS Cent Sci. 2017;3:544–53.
8. Little MA, Cooper AI. The chemistry of porous organic molecular materials. Adv Funct Mater. 2020;30:1909842.
9. Yamagishi H. Functions and fundamentals of porous molecular crystals sustained by labile bonds. Chem Commun. 2022;58:11887–97.
10. Desiraju GR. Supramolecular synthons in crystal engineering–a new organic synthesis. Angew Chem Int Ed Engl. 1995;34:2311–27.
11. Yang W, Greenaway A, Lin X, Matsuda R, Blake AJ, Wilson C, et al. Exceptional thermal stability in a supramolecular organic framework: porosity and gas storage. J Am Chem Soc. 2010;132:14457–69.
12. Chen TH, Popov I, Kaveevivitchai W, Chuang YC, Chen YS, Daugulis O, et al. Thermally robust and porous noncovalent organic framework with high affinity for fluorocarbons and CFCs. Nat Commun. 2014;5:5131.
13. Yamamoto A, Hamada T, Hisaki I, Miyata M, Tohnai N. Dynamically deformable cube-like hydrogen-bonding networks in water-responsive diamondoid porous organic salts. Angew Chem Int Ed. 2013;52:1709–12.
14. Duchamp DJ, Marsh RE. The crystal structure of trimesic acid (benzene-1,3,5-tricarboxylic acid). Acta Crystallogr Sect B. 1969;25:5–19.
15. Ermer O. Five-fold diamond structure of adamantane-1,3,5,7-tetracarboxylic acid. J Am Chem Soc. 1988;110:3747–54.
16. Simard M, Su D, Wuest JD. Use of hydrogen bonds to control molecular aggregation. self-assembly of three-dimensional networks with large chambers. J Am Chem Soc. 1991;113:4696–8.
17. Endo K, Sawaki T, Koyanagi M, Kobayashi K, Masuda H, Aoyama Y. Guest-binding properties of organic crystals having an extensive hydrogen-bonded network: an orthogonal anthracene-bis(resorcinol) derivative as a functional organic analog of zeolites. J Am Chem Soc. 1995;117:8341–52.
18. Herbstein FH, Kapon M, Reisner GM. Catenated and non-catenated inclusion complexes of trimesic acid. J Incl Phenom. 1987;5:211–4.
19. Kolotuchin SV, Fenlon EE, Wilson SR, Loweth CJ, Zimmerman SC. Self-assembly of 1,3,5-benzenetricarboxylic acids (trimesic acids) and several analogues in the solid state. Angew Chem Int Ed Engl. 1996;34:2654–7.
20. Brunet P, Simard M, Wuest JD. Molecular tectonics. porous hydrogen-bonded networks with unprecedented structural integrity. J Am Chem Soc. 1997;119:2737–8.
21. Hollingsworth MD, Santarsiero BD, Harris KDM. Zigzag channels in the structure of sebaconitrile/urea. Angew Chem Int Ed Engl. 1994;33:649–52.
22. Venkataraman D, Lee S, Zhang J, Moore JS. Hollow organic solids. Nature. 1994;371:591–3.
23. Kobayashi K, Shirasaka T, Sato A, Horn E, Furukawa N. Self-assembly of a radially functionalized hexagonal molecule: hexakis(4-hydroxyphenyl)benzene. Angew Chem Int Ed. 1999;38:3483–6.
24. Davis CJ, Lewis PT, Billodeaux DR, Fronczek FR, Escobedo JO, Strongin RM. Solid-state supramolecular structures of resorcinol−arylboronic acid compounds. Org Lett. 2001;3:2443–5.
25. Fournier JH, Maris T, Wuest JD, Guo W, Galoppini E. Molecular tectonics. use of the hydrogen bonding of boronic acids to direct supramolecular construction. J Am Chem Soc. 2003;125:1002–6.
26. Kobayashi K, Sato A, Sakamoto S, Yamaguchi K. Solvent-induced polymorphism of three-dimensional hydrogen-bonded networks of hexakis(4-carbamoylphenyl)benzene. J Am Chem Soc. 2003;125:3035–45.

27. Görbitz CH, Nilsen M, Szeto K, Tangen LW. Microporous organic crystals: an unusual case for l-leucyl-l-serine. Chem Commun. 2005;41:4288–90.
28. Miki K, Masui A, Kasai N, Miyata M, Shibakami M, Takemoto K. New channel type inclusion compound of steroidal bile acid. structure of 1:1 complex between cholic acid and acetophenone. J Am Chem Soc. 1988;110:6594–6.
29. Nakano K, Sada K, Miyata M. Inclusion compounds of cholic acid with various hydrocarbons and the crystal structure of a 1 : 1 complex of cholic acid and benzene. Chem Lett. 1994;23:137–40.
30. Miyata M, Tohnai N, Hisaki I. Crystalline host-guest assemblies of steroidal and related molecules: diversity, hierarchy, and supramolecular chirality. Acc Chem Res. 2007;40:694–702.
31. Toda F, Tanaka K, Omata T, Nakamura K, Oshima T. Optical resolution of 3-methylcycloalkanones and 5-methyl-.gamma.-butyrolactone by complexation with optically active 1,6-bis(o-halophenyl)-1,6-diphenylhexa-2,4-diyne-1,6-diol. J Am Chem Soc. 1983;105:5151–2.
32. Adachi T, Ward MD. Versatile and resilient hydrogen-bonded host frameworks. Acc Chem Res. 2016;49:2669–79.
33. Yu S, Xing GL, Chen LH, Ben T, Su BL. Crystalline porous organic salts: from micropore to hierarchical pores. Adv Mater. 2020;32:2003270.
34. Luo J, Wang JW, Zhang JH, Lai S, Zhong DC. Hydrogen-bonded organic frameworks: design, structures and potential applications. Cryst Eng Comm. 2018;20:5884–98.
35. Lin RB, He Y, Li P, Wang H, Zhou W, Chen B. Multifunctional porous hydrogen-bonded organic framework materials. Chem Soc Rev. 2019;48:1362–89.
36. Hisaki I, Xin C, Takahashi K, Nakamura T. Designing hydrogen-bonded organic frameworks (HOFs) with permanent porosity. Angew Chem Int Ed. 2019;58:11160–70.
37. Hisaki I. Hydrogen-bonded porous frameworks constructed by rigid π-conjugated molecules with carboxy groups. J Incl Phenom Macrocycl Chem. 2020;96:215–31.
38. Wang B, Lin RB, Zhang Z, Xiang S, Chen B. Design rules of hydrogen-bonded organic frameworks with high chemical and thermal stabilities. J Am Chem Soc. 2020;142:14399–416.
39. Li P, Ryder MR, Stoddart JF. Hydrogen-bonded organic frameworks: a rising class of porous molecular materials. Acc Mater Res. 2020;1:77–87.
40. Nunzio MR, Hisaki I, Douhal A. HOFs under light: relevance to photon-based science and applications. J Photochem Photobio C: Photochem Rev. 2021;47:100418.
41. Chen L, Zhang B, Chen L, Liu H, Hu Y, Qiao S. Hydrogen-bonded organic frameworks: design, applications, and prospects. Mater Adv. 2022;3:3680–708.
42. Song X, Wang Y, Wang C, Wang D, Zhuang G, Kirlikovali KO, et al. Design rules of hydrogen-bonded organic frameworks with high chemical and thermal stabilities. J Am Chem Soc. 2022;144:10663–87.
43. Lin ZJ, Mahammed SAR, Liu TF, Cao R. Multifunctional porous hydrogen-bonded organic frameworks: current status and future perspectives. ACS Cent Sci. 2022;8:1589–608. 43
44. Leiserowitz L. Molecular packing modes. carboxylic acids. Acta Crystallogr Sect B. 1976;32:775–802.
45. Ivasenko O, Perepichka DF. Mastering fundamentals of supramolecular design with carboxylic acids. common lessons from X-ray crystallography and scanning tunneling microscopy. Chem Soc Rev. 2011;40:191–206.
46. O'Keeffe M, Yaghi OM. Deconstructing the crystal structures of metal–organic frameworks and related materials into their underlying nets. Chem Rev. 2012;112:675–702.
47. Cui P, Mcmahon DP, Spackman PR, Alston BM, Little MA, Day GM, et al. Mining predicted crystal structure landscapes with high throughput crystallisation: old molecules, new insights. Chem Sci. 2019;10:9988–97.
48. Tothadi S, Koner K, Dey K, Addicoat M, Banerjee R. Morphological evolution of two-dimensional porous hexagonal trimesic acid framework. ACS Appl Mater Interfaces. 2020;12:15588–94.
49. Zentner CA, Lai HWH, Greenfield JT, Wiscons RA, Zeller M, Campana CF, et al. High surface area and Z' in a thermally stable 8-fold polycatenated hydrogen-bonded framework. Chem Commun. 2015;51:11642–5.
50. Yoon TU, Bin Baek S, Kim D, Kim EJ, Lee WG, Singh BK, et al. Efficient separation of C_2 hydrocarbons in a permanently porous hydrogen-bonded organic framework. Chem Commun. 2018;54:9360–3.
51. Yang W, Zhou W, Chen B. A flexible microporous hydrogen-bonded organic framework. Cryst Growth Des. 2019;19:5184–8.
52. Lai HWH, Wiscons RA, Zentner CA, Zeller M, Rowsell JLC. Supramolecular assembly of tris(4-carboxyphenyl)arenes: relationship between molecular structure and solid-state catenation motifs. Cryst Growth Des. 2016;16:821–33.
53. Liang R, Samanta J, Shao B, Zhang M, Staples RJ, Chen AD, et al. A heteromeric carboxylic acid based single-crystalline crosslinked organic framework. Angew Chem Int Ed. 2021;60:23176–81.
54. Nandi S, Chakraborty D, Vaidhyanathan R. A permanently porous single molecule H-bonded organic framework for selective CO_2 capture. Chem Commun. 2016;52:7249–52.
55. Yang W, Wang J, Wang H, Bao Z, Zhao JCG, Chen B. Highly interpenetrated robust microporous hydrogen-bonded organic framework for gas separation. Cryst Growth Des. 2017;17:6132–7.
56. Gao J, Cai Y, Qian X, Liu P, Wu H, Zhou W, et al. A microporous hydrogen-bonded organic framework for the efficient capture and purification of propylene. Angew Chem Int Ed. 2021;60:20400–6.
57. Cai Y, Chen H, Liu P, Chen K, Xu H, Alshahrani T, et al. Robust microporous hydrogen-bonded organic framework for highly selective purification of methane from natural gas. Micro Meso. Mater. 2023;352:112495.
58. Li YL, Alexandrov EV, Yin Q, Li L, Fang ZB, Yuan W, et al. Record complexity in the polycatenation of three porous hydrogen-bonded organic frameworks with stepwise adsorption behaviors. J Am Chem Soc. 2020;142:7218–24.
59. Li T, Liu BT, Bin Fang Z, Yin Q, Wang R, Liu TF. Integrating active C_3N_4 moieties in hydrogen-bonded organic frameworks for efficient photocatalysis. J Mater Chem A. 2021;9:4687–91.
60. Hisaki I, Emilya Affendy NQ, Tohnai N. Precise elucidations of stacking manners of hydrogen-bonded two-dimensional organic frameworks composed of X-shaped π-conjugated systems. Cryst Eng Comm. 2017;19:4892–8.
61. Ding X, Liu Z, Zhang Y, Ye G, Jia J, Chen J. Binary solvent regulated architecture of ultra-microporous hydrogen-bonded organic frameworks with tunable polarization for highly-selective gas separation. Angew Chem Int Ed. 2022;61:e202116483.
62. Ji Q, Takahashi K, Noro SI, Ishigaki Y, Kokado K, Nakamura T, et al. A hydrogen-bonded organic framework based on pyrazinopyrazine. Cryst Growth Des. 2021;21:4656–64.
63. Kubo H, Oketani R, Hisaki I. Quasi single-crystalline transformation of porous frameworks accompanied by interlayer rearrangements of hydrogen bonds. Chem Commun. 2021;57:8568–71.
64. Gao XY, Li YL, Liu TF, Huang XS, Cao R. Single-crystal-to-single-crystal transformation of tetrathiafulvalene-based hydrogen-bonded organic frameworks. Cryst Eng Comm. 2021;23:4743–7.

65. Vicent-Morales M, Esteve-Rochina M, Calbo J, Ortí E, Vitórica-Yrezábal IJ, Espallargas GM. Semiconductor porous hydrogen-bonded organic frameworks based on tetrathiafulvalene derivatives. J Am Chem Soc. 2022;144:9074–82.
66. Kirlikovali KO, Goswami S, Mian MR, Krzyaniak MD, Wasielewski MR, Hupp JT, et al. An electrically conductive tetrathiafulvalene-based hydrogen-bonded organic framework. ACS Mater Lett. 2022;4:128–35.
67. Shustova NB, McCarthy BD. Dincă M. Turn-on fluorescence in tetraphenylethylene-based metal–organic frameworks: an alternative to aggregation-induced emission. J Am Chem Soc. 2011;133:20126–9.
68. Suzuki Y, Tohnai N, Hisaki I. Triaxially woven hydrogen-bonded chicken wires of a tetrakis(carboxybiphenyl)ethene. Chem Eur J. 2020;26:17056–62.
69. Ma K, Li P, Xin JH, Chen Y, Chen Z, Goswami S, et al. Ultrastable mesoporous hydrogen-bonded organic framework-based fiber composites toward mustard gas detoxification. Cell Rep Phys Sci. 2020;1:100024.
70. Yin Q, Zhao P, Sa RJ, Chen GC, Jian L, Liu TF, et al. An ultrarobust and crystalline redeemable hydrogen-bonded organic framework for synergistic chemo-photodynamic therapy. Angew Chem Int Ed. 2018;57:7691–6.
71. Wang Y, Ma K, Bai J, Xu T, Han W, Wang C, et al. Chemically engineered porous molecular coatings as reactive oxygen species generators and reservoirs for long-lasting self-cleaning textiles. Angew Chem Int Ed Engl. 2022;61:e202115956.
72. Wang B, Lv XL, Lv J, Ma L, Lin RB, Cui H, et al. A novel mesoporous hydrogen-bonded organic framework with high porosity and stability. Chem Commun. 2020;56:66–9.
73. Hashimoto T, Oketani R, Nobuoka M, Seki S, Hisaki I. Single crystalline, non-stoichiometric cocrystals of hydrogen-bonded organic frameworks. Angew Chem Int Ed. 2023;62:e202215836.
74. Zhang H, Yu D, Liu S, Liu C, Liu Z, Ren J, et al. NIR-II hydrogen-bonded organic frameworks (HOFs) used for target-specific amyloid-β photooxygenation in an alzheimer's disease model. Angew Chem Int Ed. 2022;61:e202109068.
75. Yin Q, Lü J, Li HF, Liu TF, Cao R. Robust microporous porphyrin-based hydrogen-bonded organic framework for highly selective separation of C_2 hydrocarbons versus methane. Cryst Growth Des. 2019;19:4157–61.
76. Liu BT, Pan XH, Nie DY, Hu XJ, Liu EP, Liu TF. Ionic hydrogen-bonded organic frameworks for ion-responsive antimicrobial membranes. Adv Matter. 2020;32:2005912.
77. Yin Q, Alexandrov EV, Si DH, Huang QQ, Fang ZB, Zhang Y, et al. Metallization-prompted robust porphyrin-based hydrogen-bonded organic frameworks for photocatalytic CO_2 reduction. Angew Chem Int Ed. 2022;61:e202115854.
78. Cui P, Svensson Grape E, Spackman PR, Wu Y, Clowes R, Day GM, et al. An expandable hydrogen-bonded organic framework characterized by three-dimensional electron diffraction. J Am Chem Soc. 2020;142:12743–50.
79. Yang Z, Moriyama A, Oketani R, Nakamura T, Hisaki I. Two-dimensional porous framework assembled through hydrogen-bonds and dipole-dipole interactions. Chem Lett. 2021;50:1909–12.
80. Yang Z, Saeki A, Inoue A, Oketani R, Kamiya K, Nakanishi S, et al. Slip-stacking of benzothiadiazole can provide a robust structural motif for porous hydrogen-bonded organic rrameworks. Cryst Growth Des. 2022;22:4472–9.
81. Hashimoto T, Oketani R, Inoue A, Okubo K, Oka K, Tohnai N, et al. Statically and dynamically flexible hydrogen-bonded frameworks based on 4,5,9,10-tetrakis(4-carboxyphenyl)pyrene. Chem Commun. 2023;59:7224–7.
82. Yin Q, Li Y-L, Li L, Lü J, Liu T-F, Cao R. Novel hierarchical meso-microporous hydrogen-bonded organic framework for selective separation of acetylene and ethylene versus methane. ACS Appl Mater Interfaces. 2019;11:17823–7.
83. Bassanetti I, Bracco S, Comotti A, Negroni M, Bezuidenhout C, Canossa S, et al. Flexible porous molecular materials responsive to CO_2. CH4 and Xe stimuli. J Mater Chem A. 2018;6:14231–9.
84. Hu F, Liu C, Wu M, Pang J, Jiang F, Yuan D, et al. An Ultrastable and easily regenerated hydrogen-bonded organic molecular framework with permanent porosity. Angew Chem Int Ed. 2017;56:2101–4.
85. Wang JX, Gu XW, Lin YX, Li B, Qian G. A novel hydrogen-bonded organic framework with highly permanent porosity for boosting ethane/ethylene separation. ACS Mater Lett. 2021;3:497–503.
86. Yang W, Wang JX, Yu B, Li B, Wang H, Jiang J. A robust hydrogen-bonded organic framework with 7-fold interpenetration nets and high permanent microporosity. Cryst Growth Des. 2022;22:1817–23.
87. Takeda T, Ozawa M, Akutagawa T. Jumping crystal of a hydrogen-bonded organic framework induced by the collective molecular motion of a twisted π system. Angew Chem Int Ed. 2019;58:10345–52.
88. Wang B, He R, Xie LH, Lin ZJ, Zhang X, Wang J, et al. Microporous hydrogen-bonded organic framework for highly efficient turn-up fluorescent sensing of aniline. J Am Chem Soc. 2020;142:12478–85.
89. Yu B, Geng S, Wang H, Zhou W, Zhang Z, Chen B, et al. A solid transformation into carboxyl dimers based on a robust hydrogen-bonded organic framework for propyne/propylene separation. Angew Chem Int Ed. 2021;60:25942–8.
90. Chen X, Takahashi K, Kokado K, Nakamura T, Hisaki I. A proton conductive hydrogen-bonded framework incorporating 18-crown-6-ether and dicarboxy-*o*-terphenyl moieties. Mater Adv. 2021;2:5639–44.
91. Suzuki Y, Tohnai N, Saeki A, Hisaki I. Hydrogen-bonded organic frameworks of twisted polycyclic aromatic hydrocarbon. Chem Commun. 2020;56:13369–72.
92. Suzuki Y, Yamaguchi M, Oketani R, Hisaki I. Isomeric effect of naphthyl spacers on structures and properties of isostructural porous crystalline frameworks. Mater Chem Front. 2023;7:106–16.
93. Kobayashi K, Shirasaka T, Horn E, Furukawa N. Two-dimensional hexagonal hydrogen-bonded network with triangle-like large cavities: hexakis(4-carboxyphenyl)benzene. Tetrahedron Lett. 2000;41:89–93.
94. Zhang X, Li L, Wang JX, Wen HM, Krishna R, Wu H, et al. Selective ethane/ethylene separation in a robust microporous hydrogen-bonded organic framework. J Am Chem Soc. 2020;142:633–40.
95. Zhang X, Wang JX, Li L, Pei J, Krishna R, Wu H, et al. A rod-packing hydrogen-bonded organic framework with suitable pore confinement for benchmark ethane/ethylene separation. Angew Chem Int Ed. 2021;60:10304–10.
96. Hisaki I, Ikenaka N, Tohnai N, Miyata M. Polymorphs of layered assemblies of hydrogen-bonded hexagonal networks caused by conformational frustration. Chem Commun. 2016;52:300–3.
97. Hisaki I, Ikenaka N, Tsuzuki S, Tohnai N. Sterically crowded hydrogen-bonded hexagonal network frameworks. Mater Chem Front. 2018;2:338–46.
98. Hisaki I, Nakagawa S, Ikenaka N, Imamura Y, Katouda M, Tashiro M, et al. A series of layered assemblies of hydrogen-bonded, hexagonal networks of C_3-symmetric π-conjugated molecules: a potential motif of porous organic materials. J Am Chem Soc. 2016;138:6617–28.
99. Gomez E, Hisaki I, Douhal A. Synthesis and photobehavior of a new dehydrobenzoannulene-based HOF with fluorine atoms:

from solution to single crystals observation. Int J Mol Sci. 2021;22:4803.
100. Hisaki I, Nakagawa S, Tohnai N, Miyata MA. C_3-symmetric macrocycle-based, hydrogen-bonded, multiporous hexagonal network as a motif of porous molecular crystals. Angew Chem Int Ed. 2015;54:3008–12.
101. Hisaki I, Toda H, Sato H, Tohnai N, Sakurai H. A hydrogen-bonded hexagonal buckybowl framework. Angew Chem Int Ed. 2017;56:15294–8.
102. Hisaki I, Ikenaka N, Gomez E, Cohen B, Tohnai N, Douhal A. Hexaazatriphenylene-based hydrogen-bonded organic framework with permanent porosity and single-crystallinity. Chem Eur J. 2017;23:11611–9.
103. Hisaki I, Suzuki Y, Gomez E, Cohen B, Tohnai N, Douhal A. Docking strategy to construct thermostable, single-crystalline, hydrogen-bonded organic framework with high surface area. Angew Chem Int Ed. 2018;57:12650–5.
104. Suzuki Y, Gutiérrez M, Tanaka S, Gomez E, Tohnai N, Yasuda N, et al. Construction of isostructural hydrogen-bonded organic frameworks: limitations and possibilities of pore expansion. Chem Sci. 2021;12:9607–18.
105. Hisaki I, Suzuki Y, Gomez E, Ji Q, Tohnai N, Nakamura T, et al. Acid responsive hydrogen-bonded organic frameworks. J Am Chem Soc. 2019;141:2111–21.
106. Hisaki I, Ji Q, Takahashi K, Tohnai N, Nakamura T. Positional effects of annelated pyrazine rings on structure and stability of hydrogen-bonded frameworks of hexaazatrinaphthylene derivatives. Cryst Growth Des. 2020;20:3190–8.
107. Kobayashi M, Kubo H, Oketani R, Hisaki I. Quinoxaline-annelated hexadehydro[12]annulene: use of a new building block to construct a hydrogen-bonded hexagonal molecular network. Cryst Eng Comm. 2022;24:5036–40.
108. Shivakumar KI, Noro S, Yamaguchi Y, Ishigaki Y, Saeki A, Takahashi K, et al. A hydrogen-bonded organic framework based on redox-active tri(dithiolylidene)cyclohexanetrione. Chem Commun. 2021;57:1157–60.
109. Li P, Li P, Ryder MR, Liu Z, Stern CL, Farha OK, et al. Interpenetration isomerism in triptycene-based hydrogen-bonded organic frameworks. Angew Chem Int Ed. 2019;58:1664–9.
110. Li P, Chen Z, Ryder MR, Stern CL, Guo QH, Wang X, et al. Assembly of a porous supramolecular polyknot from rigid trigonal prismatic building blocks. J Am Chem Soc. 2019;141:12998–3002.
111. Chen X, Hu R-K, Takahashi K, Noro S, Nakamura T, Hisaki I. A proton conductive porous framework of an 18-crown-6-ether derivative networked by rigid hydrogen bonding modules. Angew Chem Int Ed. 2022;61:e202211686.
112. Hisaki I, Nakagawa S, Suzuki Y, Tohnai N. CO_2 sorption of layered hydrogen-bonded organic framework causes reversible structural changes involving four different crystalline states under ambient pressure. Chem Lett. 2018;47:1143–6.
113. Gomez E, Gutiérrez M, Cohen B, Hisaki I, Douhal A. Single crystal fluorescence behavior of a new HOF material: a potential candidate for a new LED. J Mater Chem C. 2018;6:6929–39.
114. Gomez E, di Nunzio MR, Moreno M, Hisaki I, Douhal A. Shape-persistent phenylene-ethynylene macrocycles spectroscopy and dynamics: from molecules to the hydrogen-bonded organic framework material. J Phys Chem C. 2020;124:6938–51.
115. Liu X, Yang X, Wang H, Hisaki I, Wang K, Jiang J. A robust redox-active hydrogen-bonded organic framework for rechargeable batteries. J Mater Chem A. 2022;10:1808–18.
116. Gomez E, Suzuki Y, Hisaki I, Moreno M, Douhal A. Spectroscopy and dynamics of a HOF and its molecular units: remarkable vapor acid sensing. J Mater Chem C. 2019;7:10818–32.

Yuto Suzuki studied chemistry, supramolecular chemistry, and crystal engineering in Department of Engineering and Graduate School of Engineering, Osaka University, and received his B.Eng. degree in 2018 and M.Eng. degree in 2020, respectively, from Osaka University. He moved to Graduate School of Engineering Science in 2020 and obtained his Ph.D. degree under the supervision of Professor Dr. Ichiro Hisaki from Osaka University in 2023. He started working in Mitsubishi Gas Chemical Company, Inc. in 2023.

Ichiro Hisaki received his B.Eng., M.Eng. and Ph.D. degrees from the Osaka University in 2000, 2002, and 2005, respectively, under the supervision of Professor Dr. Yoshito Tobe. After being a JSPS postdoctoral researcher in the group of Professor Dr. Atsuhiro Osuka at Kyoto University, he joined in the group of Professor Dr. Mikiji Miyata at Osaka University in 2005 as an assistant professor. In 2018, he moved to the group of Professor Dr. Takayoshi Nakamura at Hokkaido University as an associate professor. Since 2020, he has been a professor at Graduate School of Engineering Science, Osaka University.